

Lattice stability of ordered Au-Cu alloys in the warm dense matter regime

Shota Ono* and Daigo Kobayashi

Department of Electrical, Electronic and Computer Engineering, Gifu University, Gifu 501-1193, Japan

In the warm dense regime, where the electron temperature is increased to the same order of the Fermi temperature, the lattice stability of elemental metals depends on its electronic band structure as well as its crystal structure. It has been believed that the d electron excitations yield the phonon hardening as in noble metals, whereas the crystal structure symmetry can prevent phonon hardening at a specific point in the Brillouin zone as in alkali metals. Here, we extend this concept to binary alloys (Au and Cu) in the $L1_0$ and $L1_2$ structures. By performing first principles calculations on phonon dispersions, we demonstrate that warm dense alloys in the $L1_0$ and $L1_2$ structures show phonon softening and hardening behaviors, respectively. This suggests that for the $L1_0$ the effect of crystal structure symmetry overcomes that of weakened electron screening due to the d electron excitations.

Introduction. Lattice dynamics in metals is determined by the interplay between the direct ion-ion and the indirect ion-electron-ion interactions. In warm dense matter (WDM) regime realized by an incident of ultrafast laser pulse to metals, the latter is strongly modulated due to electron excitations characterized by the electron temperature T_e that is the same order of the Fermi temperature. By using the finite-temperature density-functional theory (DFT) [1], the phonon hardening has been predicted for elemental metals in the close-packed (i.e., face-centered cubic (FCC) and hexagonal close-packed) structures [2–8] and has been observed experimentally in warm dense Au [9]. For noble metals, this is because the excitation of d electrons weakens the electron screening, in turn, yielding an increase in the internal pressure [2, 3]. For free electron metals with no d bands near the Fermi level, the phonon hardening is due to an increase in the electron kinetic energy, leading to an increase in the internal pressure again [3]. Within the free-electron approximation using the central potential model, this is understood by an increase in the force constants of the first nearest neighbor (NN) sites [8]. In contrast, the phonon softening has been predicted for body-centered cubic (BCC) structure [6–8, 10]. This is intrinsic to the crystal structure symmetry: in the expression for the phonon frequency at the point N in the Brillouin zone, no contribution from the force constants of the first NN sites is present [8, 10]. These studies imply that the phonon hardening or softening properties in WDM are determined by a combined effect of the increase in the internal pressure (weakened screening) and the crystal structure symmetry. In order to study this interplay systematically, it is useful to focus on alloys that can have many crystal structures in thermal equilibrium and phase diagram as a function of ambient temperature and composition.

The ordered phases of Au-Cu alloys have been well known as described in the standard textbooks [11]: AuCu in the $L1_0$ structure (the distorted FCC structure along the c axis) and AuCu_3 and CuAu_3 in the $L1_2$ structure

[12], as shown in Fig. 1. In this paper, we study the lattice dynamics of ordered Au-Cu alloys in the WDM regime. We show that the warm dense Au-Cu alloy in the $L1_2$ structure shows the phonon hardening, whereas that in the $L1_0$ structure is unstable. The former can be explained by the weakening of the electron screening effect. On the other hand, the latter can be rationalized by the similarity of the crystal structure between $L1_0$ and BCC, that is, an instability intrinsic to the crystal structure.

The origin of the phonon softening in $L1_0$ AuCu alloy is different from that in warm dense diamond and silicon. For the latter, the phonon softening and lattice instabilities have been understood by the strengthening of the anti-bonding character between atoms created by the electron transition from the valence to the conduction bands, reducing the size of force constants significantly [13]. Recently, Yan et al. have studied the dynamical stability of warm dense tantalum nitrides (TaN) in various structures [14] using finite-temperature DFT. They have shown that under electronic excitations the unstable cubic δ -phase becomes stable, whereas the hexagonal phases show the phonon softening. They have explained it with respect to the covalent bonding between atoms in more complicated way.

Computational details. We calculate the total energy and the phonon dispersions of Au-Cu alloys based on DFT and density-functional perturbation theory [15] implemented in **Quantum ESPRESSO** (QE) code [16]. We treat the effects of exchange and correlation within GGA-PBE

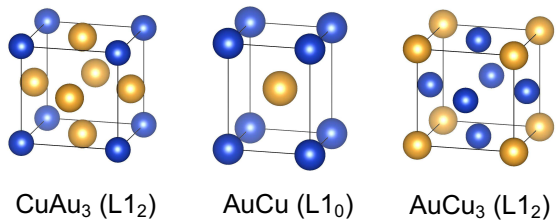


FIG. 1: Crystal structure of CuAu_3 ($L1_2$), AuCu ($L1_0$), and AuCu_3 ($L1_2$).

*Electronic address: shota_o@gifu-u.ac.jp

[17] and PBEsol [18] and use the ultrasoft pseudopotentials provided in `pslibrary.1.0.0` [19]. The cutoff energies for the wavefunction and the charge density are 80 Ry and 800 Ry, respectively. The self-consistent field and phonon dispersion calculations are performed by using $15 \times 15 \times 15$ k grid and $4 \times 4 \times 4$ q grid [20], respectively, which are enough to study the dynamical stability of warm dense alloys. The Marzari-Vanderbilt smearing [21] with a broadening of $\sigma = 0.02$ Ry is used for the geometry optimization, while the Fermi-Dirac type smearing is used for WDM regime. The tetrahedron method is used to calculate the electron density-of-states (DOS) [22]. For WDM regime, the number of electronic bands to be calculated is increased to three times larger than the sizes in the ground state calculations in order to take into account the occupation of electronic states far above the Fermi level. Imaginary phonon energies $\hbar\omega$ (\hbar the Planck constant and ω the phonon frequency) are represented by negative energies below.

PBE versus PBEsol. It has been known that the PBE functional underestimates the cohesive energy for Au-Cu alloys within the PBE [23]. Before studying the stability of warm dense alloys, we investigate whether the dynamical stability of the L1₀ structure can be described within the PBE and PBEsol. Figure 2 shows the phonon dispersion curves of AuCu in the L1₀ structure at $k_B T_e = 0$ eV (k_B the Boltzmann constant). When the PBE functional is used, the imaginary energies are observed around the point R. This would be attributed to an inadequacy of the PBE functional for describing the AuCu properties [23]. We thus use the PBEsol functional below. The optimized lattice parameter a are as follows: within the PBEsol $a = 4.069, 3.961, 2.792$ ($c/a = 1.298$), 3.711, and 3.568 Å for Au, CuAu₃, AuCu, AuCu₃, and Cu, respectively. Within the PBE, $a = 2.889$ Å ($c/a = 1.251$) for AuCu. These parameters agree with the values listed in Ref. [24]. For more accuracy, it may be better to use HSE pseudopotential [23] or random phase approximation [24] for describing the structural properties of Au-Cu alloys. However, such investigations are beyond the scope of this work.

Phonon dispersions. First of all, we show the phonon dispersion curves of warm dense Au and Cu in Fig. 3, where the electron temperature is assumed to be $k_B T_e = 0, 4$, and 6 eV. Both simple metals show the phonon hardening when T_e is increased, which is consistent with the previous calculations [2, 6]. The size of the phonon energy enhancement in Cu is large compared to that in Au. This is attributed to the different width of the d band peak in the electron DOS, which will be shown in Fig. 6 below. In addition, the phonon energy enhancement against T_e in Au seems to be smaller than that reported in Refs. [2, 6], which may be due to the different functional used in the DFT calculations.

Figure 4 shows the phonon dispersion curves of AuCu₃ and CuAu₃ in the L1₂ structure. For both alloys, the phonon hardening behaviors are also observed when T_e is increased. However, as shown in Fig. 5, L1₀ AuCu

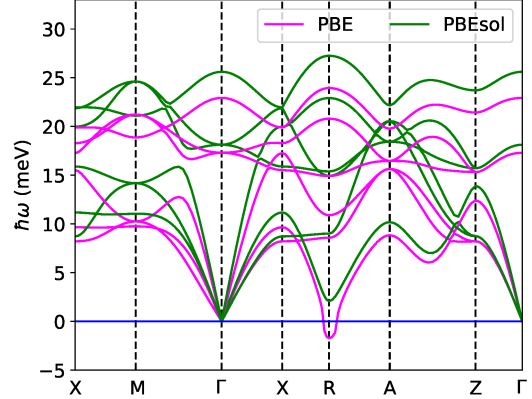


FIG. 2: Comparison of the phonon band structure of L1₀ AuCu within PBE and PBEsol. The value of T_e is set to zero.

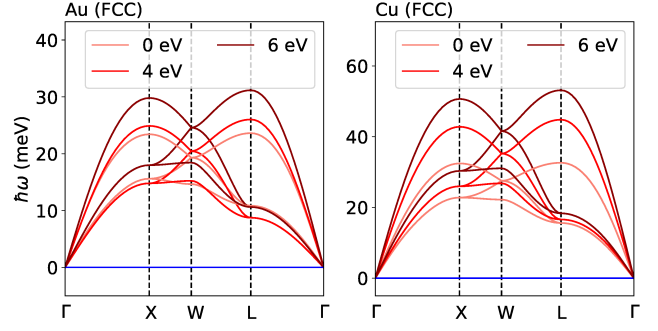


FIG. 3: The phonon band structure of Au and Cu in the FCC structure for $k_B T_e = 0, 4$, and 6 eV.

becomes unstable against T_e . While the longitudinal acoustic and optical phonons are hardened, the transverse acoustic mode is unstable because near the point R the phonon energy is imaginary.

Effect of electron screening. In order to understand the origin of the phonon hardening and softening in Au-Cu alloys, we show the electron DOS of Au, CuAu₃, AuCu, AuCu₃, and Cu in Fig. 6. At $T_e = 0$, due to the presence of d bands, the high DOS is observed below the Fermi level from -2 to -8 eV. The width becomes narrower (from -2 to -6 eV) when the Cu concentration is increased. When T_e is increased, the peak position and the width become deep and small, respectively. This can be explained as follows: when the d electrons are excited, the electron screening is weakened. This will produce bared ions, leading to the peak shift and shrinkage of the width. This concept has been used to explain the phonon hardening in Au [2, 9]. The small increase in the phonon energy for Au observed in Fig. 3 (at $k_B T_e = 4$ eV) can be rationalized by the small change in the DOS against T_e . While varies in size, we emphasize that the

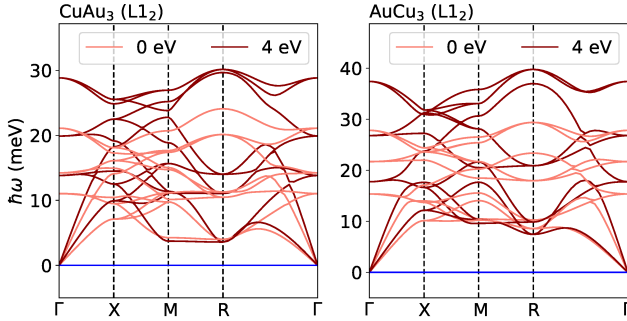


FIG. 4: The phonon band structure of CuAu₃ and AuCu₃ in the L1₂ structure for $k_B T_e = 0$ and 4 eV.

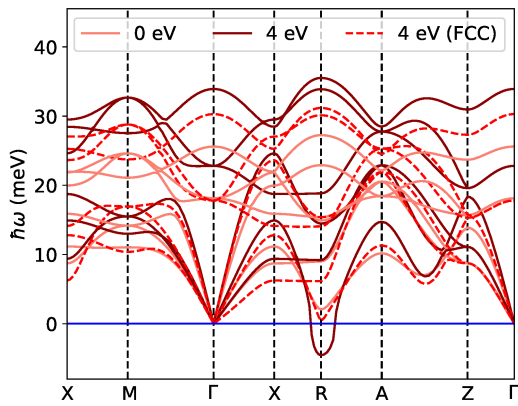


FIG. 5: The phonon band structure of AuCu in the L1₀ structure for $k_B T_e = 0$ and 4 eV (solid). The dashed curves indicate the case of AuCu in the FCC structure for $k_B T_e = 4$ eV.

change in the electron DOS of Au-Cu alloys reflects the d electron excitations. Therefore, the phonon hardening in Au-Cu alloys can be attributed to the weakened electron screening that leads to an increase in the internal pressure, as in noble metals and Al [3, 4, 8]. In this sense, the phonon softening behavior observed in L1₀ AuCu is quite strange.

Effect of crystal structure symmetry. The L1₀ structure is formed by stacking the square lattices of different elements (Au and Cu) along the (001) direction alternately. With the square lattices of the same elements assumed, the L1₀ structure is exactly the same as the BCC (or B2) structure ($c/a = 1$) and the FCC structure ($c/a = \sqrt{2}$). In the BCC metals, the phonon softening occurs at the point N, $(0, \pi/a, \pi/a)$, because the dynamical matrix does not include the force constants from the first NN sites due to the crystal symmetry [8]. The point N is near the point R in the L1₀ structure, $(0, \pi/a, \pi/c)$, because $c/a = 1.298$. Therefore, the softening behavior in the L1₀ structure can be explained as in the case

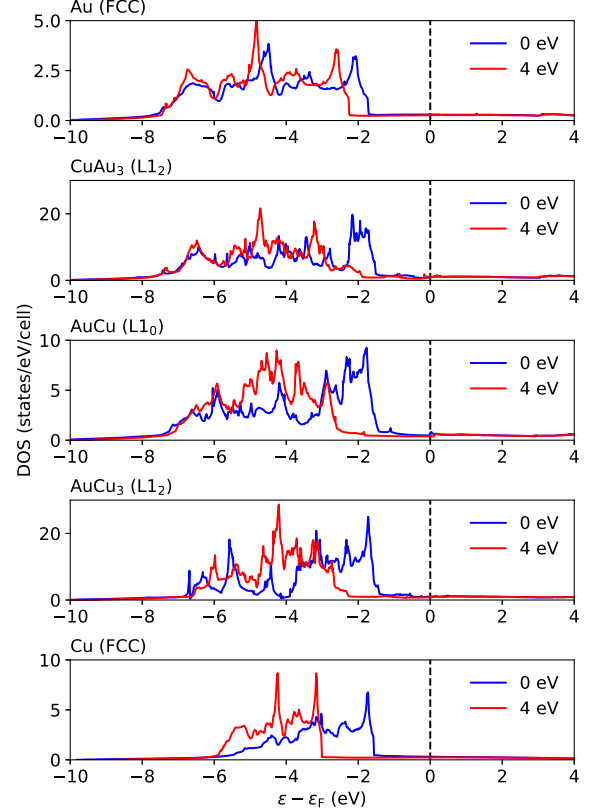


FIG. 6: The electron DOS for Au, CuAu₃, AuCu, AuCu₃, and Cu for $k_B T_e = 0$ eV and 4 eV. The electron energy is measured from the Fermi level.

of the BCC metals. In order to confirm the validity of this hypothesis, we have calculated the phonon dispersion curves of FCC AuCu at $k_B T_e = 4$ eV by increasing c/a up to $\sqrt{2}$, similarly to the Bain distortion [25]. In fact, the AuCu alloy recovers the lattice stability, as shown in Fig. 5, while the size of the highest phonon energy decreases since the volume of the unit cell is increased.

We present a qualitative discussion of the instability at the point R by using the symmetry property of the L1₀ structure. The dynamical matrix for the wavevector \mathbf{q} is defined as

$$\tilde{D}_{\alpha\alpha'}^{ss'}(\mathbf{q}) = \sum_{\mathbf{R}} D_{\alpha\alpha'}^{ss'}(\mathbf{R}) e^{i\mathbf{q}\cdot\mathbf{R}} \quad (1)$$

with the polarization α , and the lattice vector \mathbf{R} that characterizes the unit cell including the atoms s . We consider the contribution from the first NN sites only, which would be significant in determining the stability of metals [4]. Without loss of generality, we then focus on the force on eight Cu atoms around the Au atom at the origin when the latter is displaced. With s and s'

being Cu and Au, respectively, the superscript is omitted below. At the point R, one obtains

$$\tilde{D}_{\alpha\alpha'}(\mathbf{q}) = \sum_{l=1,4,6,7} D_{\alpha\alpha'}(\mathbf{R}_l) - \sum_{l=2,3,5,8} D_{\alpha\alpha'}(\mathbf{R}_l), \quad (2)$$

where the lattice vectors \mathbf{R}_l is given by $\mathbf{R}_{4n+1} = (0, 0, -cn)$, $\mathbf{R}_{4n+2} = (-a, 0, -cn)$, $\mathbf{R}_{4n+3} = (0, -a, -cn)$, and $\mathbf{R}_{4n+4} = (-a, -a, -cn)$ with $n = 0, 1$ by assuming the basis vector $\tau = (a/2, a/2, c/2)$. For the L1₀ structure, there are 16 symmetry operations \mathcal{S} including the identity, 180 degree rotation around x, y, z , and $[1, \pm 1, 0]$ axis, ± 90 degree rotation around z axis, and the inversions. Due to the symmetry property, the following relation holds [26]

$$D_{\alpha\alpha'}(\mathcal{S}\mathbf{R}) = \sum_{\mu, \mu'} S_{\alpha\mu} S_{\alpha'\mu'} D_{\mu\mu'}(\mathbf{R}) \quad (3)$$

with $S_{\alpha\mu}$ being the matrix element of \mathcal{S} . For example, $D_{xz}(\mathbf{R}_1) = -D_{xz}(\mathbf{R}_2) = D_{xz}(\mathbf{R}_3) = -D_{xz}(\mathbf{R}_4) = -D_{xz}(\mathbf{R}_5) = D_{xz}(\mathbf{R}_6) = -D_{xz}(\mathbf{R}_7) = D_{xz}(\mathbf{R}_8)$. With these restrictions on the dynamical matrix, the equality $\tilde{D}_{\alpha\alpha'}(\mathbf{q}) = 0$ holds exactly within the first NN approximation: Cu (Au) atoms vibrate as if they are decoupled with Au (Cu) atoms. This implies that the R point phonon should be stabilized by the second or higher order NN interactions at $T_e = 0$. The size of such matrix elements is expected to be small compared to that for the first NN sites, giving rise to small phonon energies in Figs. 2 and 5. Since in the WDM regime the phonon hardening is mainly due to the increase in the first NN interaction [4, 8], no phonon hardening occurs at the point R. Furthermore, due to the absence of the Friedel-like oscillation for the interatomic potential in the WDM regime [7, 8], the magnitude and even the sign of the force constants from the higher order NN sites will be modulated and flipped, respectively, giving rise to the instability of AuCu in the L1₀ structure.

Summary. We have studied the dynamical stability of Au-Cu alloys in the WDM regime by calculating the phonon dispersion curves. The phonon hardening and softening are observed in the L1₂ and L1₀ structures, respectively. The former can be explained by the increase in the internal pressure caused by the d electron excitations, as observed in noble metals. On the other hand, the instability of L1₀ structure against the R point phonon excitation is intrinsic to its crystal structure, similar to the phonon softening at the point N in the BCC metals. The interplay between these factors will be a key to understand the lattice stability of more complex alloys in the WDM regime.

It is valuable to note that 51 L1₀ and 294 L1₂ alloys are found in experimental phase diagrams [27]. In the WDM regime, they will show the phonon softening and hardening, respectively, whereas we will not expect that alloys in the L1₀ structure with $c/a \simeq \sqrt{2}$ (e.g., AlTi) become unstable against moderate T_e , as shown in Fig. 5. In addition, the stability property of 325 B2 alloys [27] at high T_e will be the same as that of the L1₀ alloys with small $c/a \simeq 1$. It is interesting to perform high-throughput calculations on how the phonon hardening and softening behaviors depend on the structural parameters.

Finally, it should be noted that the WDM is a transient phase because the excited electron energy created by a laser pulse is transferred to phonons, leading to lattice disordering or melting within a few picoseconds [28–30]. It is thus desirable to simulate the time-evolution of lattice displacements in warm dense alloys accurately, which enables us to interpret time-resolved experiments.

Acknowledgments

A part of numerical calculations has been done using the facilities of the Supercomputer Center, the Institute for Solid State Physics, the University of Tokyo.

[1] N. D. Mermin, Thermal properties of the inhomogeneous electron gas, *Phys. Rev.* **137**, A1441 (1965).

[2] V. Recoules, J. Clérouin, G. Zérah, P. M. Anglade, and S. Mazevet, Effect of Intense Laser Irradiation on the Lattice Stability of Semiconductors and Metals, *Phys. Rev. Lett.* **96**, 055503 (2006).

[3] F. Bottin and G. Zérah, Formation enthalpies of mono-vacancies in aluminum and gold under the condition of intense laser irradiation, *Phys. Rev. B* **75**, 174114 (2007).

[4] F. C. Kabeer, E. S. Zijlstra, and M. E. Garcia, Road of warm dense noble metals to the plasma state: Ab initio theory of the ultrafast structural dynamics in warm dense matter, *Phys. Rev. B* **89**, 100301(R) (2014).

[5] D. V. Minakov and P. R. Levashov, Melting curves of metals with excited electrons in the quasiharmonic approximation, *Phys. Rev. B* **92**, 224102 (2015).

[6] G. Q. Yan, X. L. Cheng, H. Zhang, Z. Y. Zhu, and D. H. Ren, Different effects of electronic excitation on metals and semiconductors, *Phys. Rev. B* **93**, 214302 (2016).

[7] L. Harbour, M. W. C. Dharma-wardana, D. D. Klug, and L. J. Lewis, Equation of state, phonons, and lattice stability of ultrafast warm dense matter, *Phys. Rev. E* **95**, 043201 (2017).

[8] S. Ono, Lattice dynamics for isochorically heated metals: A model study, *J. Appl. Phys.* **126**, 075113 (2019).

[9] R. Ernstorfer, M. Harb, C. T. Hebeisen, G. Sciaiani, T. Dartigalongue, R. J. D. Miller, The Formation of Warm Dense Matter: Experimental Evidence for Electronic Bond Hardening in Gold, *Science* **323**, 1033 (2009).

[10] S. Ono and D. Kobayashi, Phonon softening in sodium with a stepwise electron distribution, *J. Appl. Phys.* **127**, 165105 (2020).

[11] C. Kittel, *Introduction to Solid State Physics*, 8th edition (Wiley, Hoboken, NJ, 2005).

[12] H. Okamoto, D. J. Chakrabarti, D. E. Laughlin, and T. B. Massalski, The Au-Cu (Gold-Copper) System, *J. Phase Equilib.* **8**, 454 (1987).

[13] P. Stampfli and K. H. Bennemann, Theory for the instability of the diamond structure of Si, Ge, and C induced by a dense electron-hole plasma, *Phys. Rev. B* **42**, 7163 (1990).

[14] G. Q. Yan, X. L. Cheng, and H. Zhang, Phase stability and mechanical response of tantalum nitrides to electronic excitation effect, *Mater. Res. Express* **7**, 066508 (2020).

[15] S. Baroni, S. Gironcoli, A. D. Corso, and P. Giannozzi, Phonons and related crystal properties from density-functional perturbation theory, *Rev. Mod. Phys.* **73**, 515 (2001).

[16] P. Giannozzi *et al.*, Advanced capabilities for materials modelling with Quantum ESPRESSO, *J. Phys.: Condens. Matter* **29**, 465901 (2017).

[17] J. P. Perdew, K. Burke, and M. Ernzerhof, Generalized Gradient Approximation Made Simple, *Phys. Rev. Lett.* **77**, 3865 (1996).

[18] J. P. Perdew, A. Ruzsinszky, G. I. Csonka, O. A. Vydrov, G. E. Scuseria, L. A. Constantin, X. Zhou, and K. Burke, Restoring the Density-Gradient Expansion for Exchange in Solids and Surfaces, *Phys. Rev. Lett.* **100**, 136406 (2008).

[19] A. Dal Corso, Pseudopotentials periodic table: From H to Pu, *Computational Material Science* **95**, 337 (2014).

[20] H. J. Monkhorst and J. D. Pack, Special points for Brillouin-zone integrations, *Phys. Rev. B* **13**, 5188 (1976).

[21] N. Marzari, D. Vanderbilt, A. De Vita, and M. C. Payne, Thermal Contraction and Disordering of the Al(110) Surface, *Phys. Rev. Lett.* **82**, 3296 (1999).

[22] P. E. Blöchl, O. Jepsen, and O. K. Andersen, Improved tetrahedron method for Brillouin-zone integrations, *Phys. Rev. B* **49**, 16223 (1994).

[23] Y. Zhang, G. Kresse, and C. Wolverton, Nonlocal First-Principles Calculations in Cu-Au and Other Intermetallic Alloys, *Phys. Rev. Lett.* **112**, 075502 (2014).

[24] N. K. Nepal, S. Adhikari, J. E. Bates, and A. Ruzsinszky, Treating different bonding situations: Revisiting Au-Cu alloys using the random phase approximation, *Phys. Rev. B* **100**, 045135 (2019).

[25] G. Grimvall, B. Magyari-Köpe, V. Ozolinš, and K. A. Persson, Lattice instabilities in metallic elements, *Rev. Mod. Phys.* **84**, 945 (2012).

[26] A. Maradudin, *Theory of Lattice Dynamics in the Harmonic Approximation* (Academic Press, New York, 1971).

[27] M. Sluiter, Some observed bcc, fcc, and hcp superstructures, *Phase Transitions* **80**, 299 (2007).

[28] B. I. Cho, T. Ogitsu, K. Engelhorn, A. A. Correa, Y. Ping, J. W. Lee, L. J. Bae, D. Prendergast, R. W. Falcone, and P. A. Heimann, Measurement of electron-ion relaxation in warm dense copper, *Sci. Rep.* **6**, 18843 (2016).

[29] N. Jourdain, L. Lecherbourg, V. Recoules, P. Renaudin, and F. Dorchies, Electron-ion thermal equilibration dynamics in femtosecond heated warm dense copper, *Phys. Rev. B* **97**, 075148 (2018).

[30] N. A. Smirnov, Copper, gold, and platinum under femtosecond irradiation: Results of first-principles calculations, *Phys. Rev. B* **101**, 094103 (2020).